A Distributed Sensor Network for the Ocean's Bottom Boundary Layer

A White Paper

Kurt Polzin, Joe Kuehl and Vitalii Sheremet

Abstract

The deep ocean represents a vast storehouse of heat, carbon and nutrients. These stores are accessed through the agency of *mixing across* density surfaces and *stirring along* sloping density surfaces. Stirring and mixing are typically accomplished by different sets of processes: mixing through breaking internal waves and shear instabilities, and stirring by mesoscale eddies or various frontal instabilities. Both are very strongly enhanced and become dynamically intertwined at the ocean boundaries. However, our lack of understanding of these processes limits our ability to provide advice in the context of actionable information. Our knowledge gap is especially acute as concerns mixing and stirring over steep and rough topography. In such situations the issue is that the bottom boundary conditions are directly coupled into gravity, energizing both internal waves and stratified turbulence. The excitation of gravity waves permits the efficient radiation of momentum and energy away from the boundary and provides a fast time scale restratification processes that keeps the bottom boundary layer from being well mixed, in contrast to four decades of conventional wisdom cemented in conceptual models. The crux of the issue is lack of observational ground truth.

We present a Distributed Sensor Network for the Ocean's Bottom Boundary Layer whose goal is to transcend this knowledge boundary as concerns the physics. The sensor network will enable direct estimates of momentum, energy and buoyancy fluxes in both turbulent and internal wavebands and provide the where with all for that distinction. Specific objectives are to develop a phenomenological understanding of the near-boundary physics, dense water production in gravity currents, upwelling of dense water and boundary modification of potential vorticity. A specific goal is an understanding of the role of 'friction' in the context of Earth system behavior. There is obvious collateral damage as concerns developing greater understanding of ecosystem dynamics and the carbon cycle.

Exploitation of these sensor network capabilities is in the best interest of humankind in predicting and addressing its upcoming global climate disaster. However, the current status of funding that could support such an endeavor is agency parochial, nationalistic, inefficient and inadequate to address the challenge. We envision a better future. Equally as fundamental as the Sensor Network's intellectual potential is the opportunity to develop an international community level effort that both directs, funds and mines the observations.

1 Introduction

Over decades, the paradigm in ocean observing has shifted to address the needs/understanding of the ocean community with shifts in available technology. The 1960s and 70s saw a shift from discrete water sampling with bottles to near-continuous vertical profiling of temperature and salinity and velocity, near continuous in time sampling from large costly sensors at a single location (moorings) and the development of ocean turbulence measurements on a variety of platforms. Several decades later one finds the deployment of fleets of autonomous floats (ARGO) and gliders that have, in a cost-effective way, dramatically increased sampling of the ocean interior. Similarly profound are radar arrays and satellite observations permitting unprecedented spatial analysis of the surface data and coupling of those data with high performance computing. These observing tools increasingly document the connectivity between scales that is at the heart of some of the most pressing open question(s): i.e. climate change, open-coastal ocean connectivity (upwelling-downwelling), etc.

build out this list

However, there is a key gap in knowledge required to address these open questions. This gap centers on our lack of understanding of the oceanic bottom boundary layer. This white paper presents a distributed sensor network for observing the ocean's bottom boundary layer that addresses this knowledge gap. The sensor network consists of tilt current meters that sense the ocean velocity within a meter of the seabed and are deployed along lines much as bait in long-line fishing and acoustic travel time current meters deployed on conventional taut wire moorings and bottom landers that provide estimates of turbulence and turbulent fluxes. The sensor network can be augmented with other physical sensors, such as high precision pressure instruments, for direct estimates of energy conversion rates associated with flow-topography interactions, and/or bio-geochemical sensors.

The problem we describe, that of physical transformations at the ocean's bottom boundary, is a future grand challenge that will occupy an entire generation of oceanographers. Our lack of understanding is particularly acute as concerns the role of steep and rough topography, which is where such transformations substantially take place. We have the tools for this. The major obstacle is one of funding to ignite and sustain forward progress. In this there are issues: the needs transcend the resources of a single US funding agency. The issues involve global climate. There are significant international resources, but these are not coordinated in an efficient way.

–JK Put the other aspects of bio-geochemistry, oxygen, carbon, methane, etc after this statement of specific grand challenge

In Section 2 we describe these individual components and discuss how array assets are deployed in a manner such as to achieve unprecedented spatial and temporal resolution. In Section 3 we present, in a structured fashion, how sensor network assets can address the transformation of momentum, buoyancy, energy and potential vorticity at the ocean's bottom boundary. In Section 4 we a more intuitive discussion of the science objectives as they intersect with phenomenology. In Section 5 we discuss issues and needs of current state of the art global numerical modeling and

potential intersections/engagement with high performance computing. We offer a prayer for our collective future in Section 6.

2 The Tool Kit

2.1 The Distributed Sensor Network

The Distributed Sensor Network is proven technology having evolved over 5 decades of development. What is unique in this application is the insight that network assets can be deployed to assess the issue of potential vorticity modification at the ocean's bottom boundary.

–JK This wants to be more general. Like we can do a lot with this network: including, time dependent hydraulics, internal wave generation, mixing, etc...–

We propose a network consisting of:

- 3 short (300 m tall) conventional moorings, populated with 8 MAVS current meters placed at 5-275 m Hab and O(50) self-contained temperature recorders each, will provide high vertical resolution of internal wave and outer turbulent boundary layers. These MAVS are modified to record serial data from a temperature sensor that is placed within the measurement volume of the current meter and provided with external battery packs that enable 12 months of sampling at 10 Hz. Due to the presence of chain and releases, the bottom most sensor is a 5 m height above bottom.
- Ten 10 km long, Tilt CurrentMeter (TCM) "long-line" moorings will be deployed to resolve the spatial gradients associated with the largest scale bottom boundary layer processes, those due to complex topography. This novel mooring concept provides a unique and cost-effective way for obtaining high horizontal resolution data coverage at the large length scales associated with complex topography.
- A tripod bottom lander populated by 8 MAVS current meters measuring at 0.5 and 2.5 m Hab will provide high vertical resolution of the turbulent boundary layer and directly quantify frictional stress. Bottom landers will be deployed in combination with the conventional moorings.

A conceptual rendition of distributed sensor network assets appears in figure 1.

Deployment length for convergence of statistics

2.2 Methods: The Modular Acoustic Velocity Sensor, MAVS

The travel time technology behind the MAVS was originally developed by Sandy Williams as the Benthic Acoustic Stress Sensor (*Williams 3rd et al.*, 1987) deployed on stable bottom landers (*Shaw et al.*, 2001), and for differential flow (vertical shear) measurements on nearly neutrally-buoyant floats (*Kunze et al.*, 1990; *Sun et al.*, 1996). This technology has been used for studies of turbulence and turbulent fluxes as part of instrument packages deployed on weighted wires from holes drilled through an ice shelf (*Davis and Nicholls*, 2019) and from buoys moored into sea ice

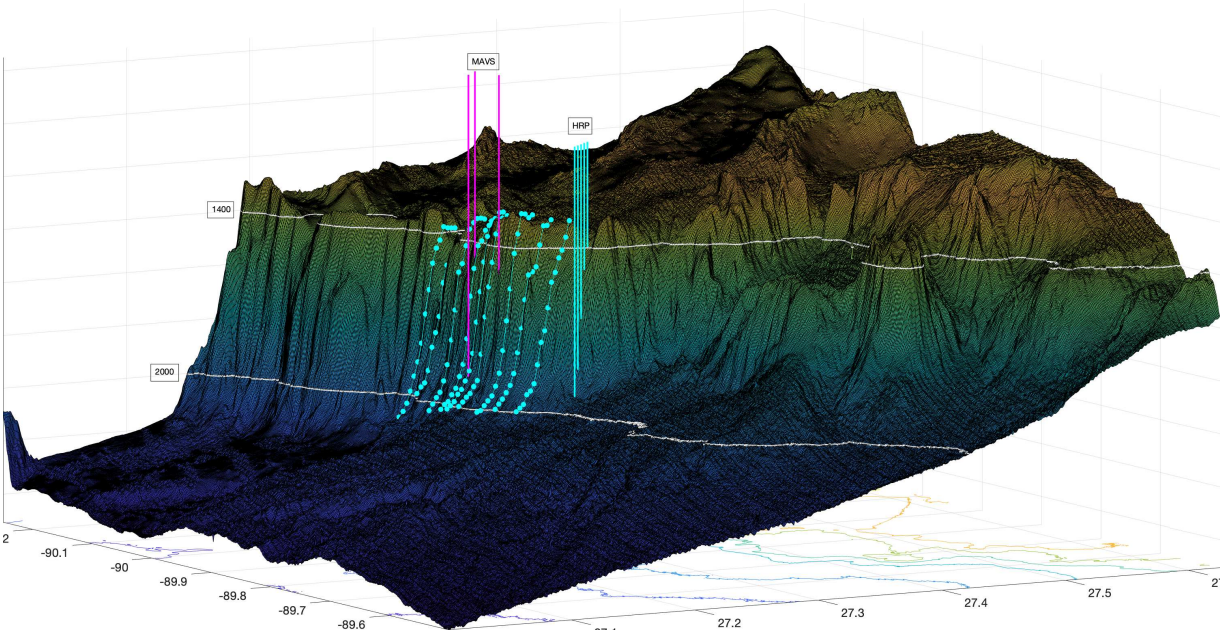

Figure 1: The Distributed Sensor Network with proposed assets deployed over a deepwater escarpment in the Gulf of Mexico.

(*Cole et al.*, 2017). This acoustic travel time technology provides a 3-D velocity estimate having a nominal precision of a few tenths of a mm s^{-1}. In practice, noise levels are speed-dependent and likely associated with flow distortion resulting from the rings holding the transducers (Fig. 2). This appears as a white noise floor of 0.3-0.6 cm s^{-1}, with noise in the vertical velocity component less than the horizontal components. Unlike a conventional Janus Doppler system, it provides a point measurement enabling a spatially co-located estimate of temperature and/or buoyancy flux.

Polzin et al. (2021) report a novel attempt to utilize a turbulence flux sensor (MAVS) on a conventional mooring. This mooring was deployed in the Gulf of Mexico in the immediate lee of a ridge on top of a prominence immediately to the east of the Mississippi Canyon. During this deployment near-bottom currents were approximately 0.2 m s^{-1} in a downwelling favorable configuration. These data document many of the features expected of a stratified Ekman layer: a buoyancy anomaly over a height less than that of the unstratified Ekman layer and an enhanced turning of the velocity vector with depth. Turbulent stress estimates have an appropriate magnitude and are aligned with the near-bottom velocity vector.

However, the Ekman layer was time dependent on inertial-diurnal time scales. Cross slope momentum and temperature fluxes have significant contributions from this frequency band. Collocated turbulent kinetic energy dissipation and temperature variance dissipation estimates imply a dissipation ratio of 0.14 that are not sensibly different from canonical values for shear instability (0.2). This mixing signature is associated with production in the internal wave band rather than frequencies associated with turbulent shear production. In general, their results do not support recent theoretical assumptions concerning 1-dimensional models of boundary mixing.

The authors regard the internal wave band fluxes as representing a direct coupling of the boundary layer to internal waveband processes and further remark that the expectation of a quasi-stationary response to quasi-stationary forcing in the guise of eddy variability is naive.

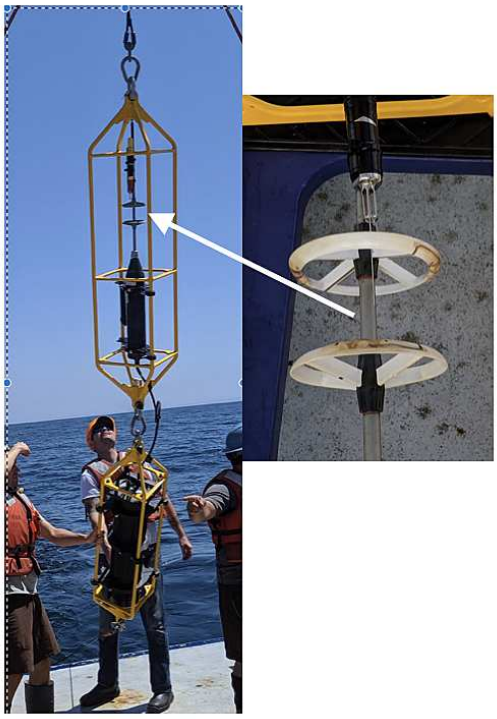

Figure 2: Left: MAVS current meter and external battery. Right: temperature probe placed within the 7 cm cubed sensing volume of the MAVS.

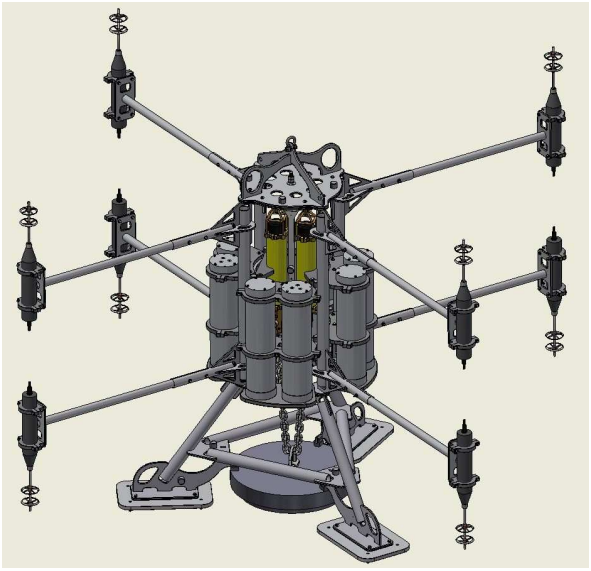

Figure 3: The bottom lander. MAVS current meters are placed in each quadrant to ensure sampling water undisturbed by the lander's structure. Sensor heads are at a nominal 0.5 and 2.5 m height above bottom.

The application of this technology is thus capable of ground-breaking and transformative research. Remaining engineering challenges are discussed in an appendix. These concern power and data storage solutions to permit year-long time series of turbulence and turbulent fluxes and sampling rate solutions to enhance signal-to-noise ratios at high flow speeds.

2.3 Methods: Tilt Current Meter Strings

TCMs are an emerging, yet proven, technology for low-cost measurement of horizontal velocity and temperature, developed by Co-PI Sheremet (via ONR and NOAA funding). The basic SeaHorse TCM instrument consists of a one-meter buoyant tube, three-axes accelerometer, three-axis magnetometer and temperature sensor. The unit is tethered to a base plate/weight and velocity is calculated based on the tilt of the instrument through well-established drag laws. The SeaHorse TCM has been compared to other current meters (such as ADVs and ADCPs, *Aretxabaleta et al.* (2014); figure 6) and shown to give accurate velocity reading from approximately 0-100cm/s with theoretical resolution of roughly 0.1 cm/s with high temporal recording frequencies (1-8Hz, though burst sampling at 8Hz for 10s each minute is more common). A deep-water version of the classic Seahorse TCM has been developed as part of the NOPP program and has shown great promise for probing the deep ocean. In general, TCM performance improves with depth. Finer tuning of TCM ballast and drag calibrations becomes possible increasingly uniform background stratification.

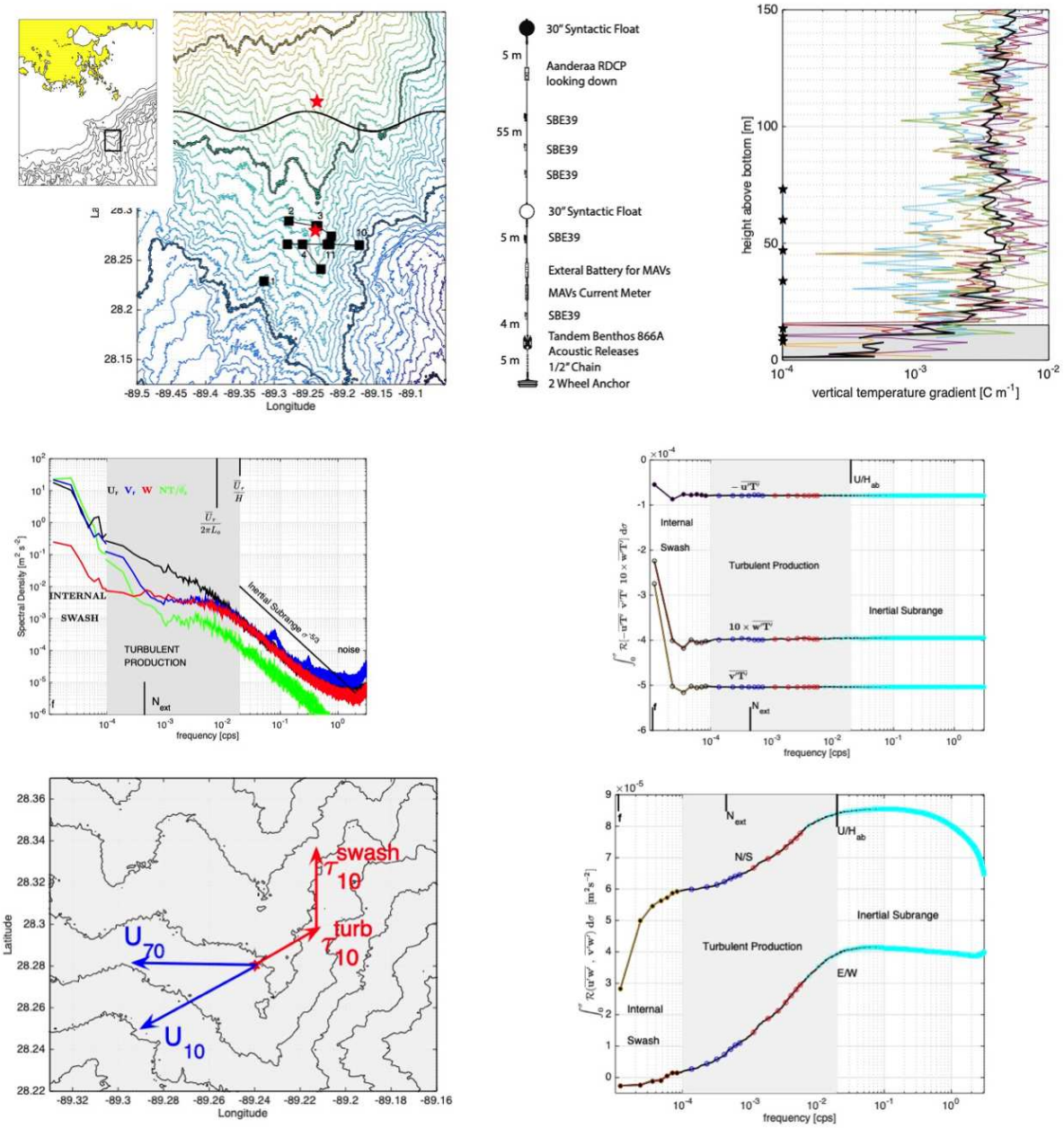

Figure 4: The relevant figures from *Polzin et al.* (2021). Walk the reader through the arguments that nonlinear transports are needed to connect fluxes to the inertial subrange and also to close a temperature variance budget. The limitations of this proof of concept study are its short time duration which renders flux and nonlinear transport estimates to be uncertain and the lack of vertical resolution. However, later studies (as of yet unpublished data) provide clear evidence of up-gradient buoyancy fluxes and far more robust estimates of nonlinear transports.

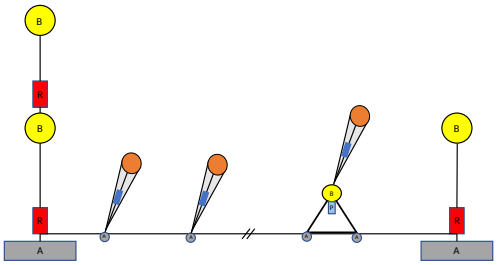

Figure 5: Schematic drawing of TCM "long-line" bottom mooring. B = buoyancy, R = acoustic release, A = anchor, P = pressure sensor (optional), Blue rectangles are tilt sensors. Note, figure is not to scale.

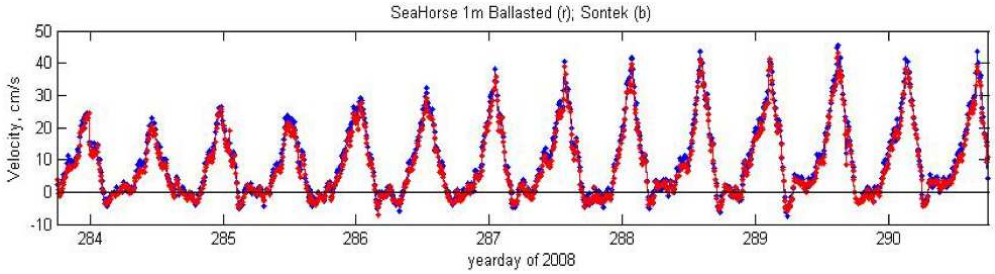

Figure 6: Comparison between Sontek Argonaut (blue) and SeaHorse TCM (red)

2.4 Methods: Direct estimates of energy flux $\overline{p'\mathbf{u}'}$

Take lots of temeprature sensors taped to a mooring cable, use these to integrate the hydrostatic approximation and set the bottom integration constant with Bottom Pressure Recorders in rocket launchers on anchors.

2.5 Methods: Bottom Pressure Torque

The traditional approach to bottom pressure torque concepts relies on taking the curl of the depth averaged steady horizontal momentum equations *Hughes and De Cuevas* (2001). After some algebraic manipulations, applying relevant approximations and physical reasoning, one reaches statements suggesting that the wind stress curl can be balanced by bottom pressure torque ($\nabla P_b \times \nabla H$ with P_b the bottom pressure and H representing water column depth due to topography) alone in the western boundary (or the circumpolar polar) current without the need for frictional effects (aka the classic Stommel, Munk, and inertial scaling). Indeed, *Ierley and Sheremet* (1995) considered a single gyre wind driven circulation and found that without the bottom drag and with the lateral friction only, the solution exhibits the inertial runaway: gyre scale circulation becomes unrealistically strong, speeds 50m/s, for fairly minor changes in the lateral friction. Basically, some mechanism is missing from the traditional quasi-geostrophic equations to balance basin averaged wind stress torque. The bottom pressure torque *Holloway and Rhines* (1991); *Ponte and Rosen* (1994); *Cane et al.* (1998) is a possibility, but other options do exist, for example, the wave drag. In the western boundary currents, internal waves are generated at the thermocline due to shear instability and carry momentum downward; thus, producing drag on the western boundary current *Ierley* (1990). This open question stems from our poor knowledge of the near bottom currents, specifically their spatio-temporal variability at internal wave frequencies. The deep near bottom observations are scarce and often technically impossible by acoustic current profilers due to the blanking distance. It is not clear how much the near surface currents (like ocean gyres or the circumpolar current) penetrate below the thermocline, which determines the bottom drag and the torque balance on the circulation. By measuring near bottom current spatio-temporal fluctuations at internal wave periods, we will directly resolve the bottom drag, and by measuring both velocity and pressure fluctuation, we will directly resolve the momentum flux (drag) due to waves.

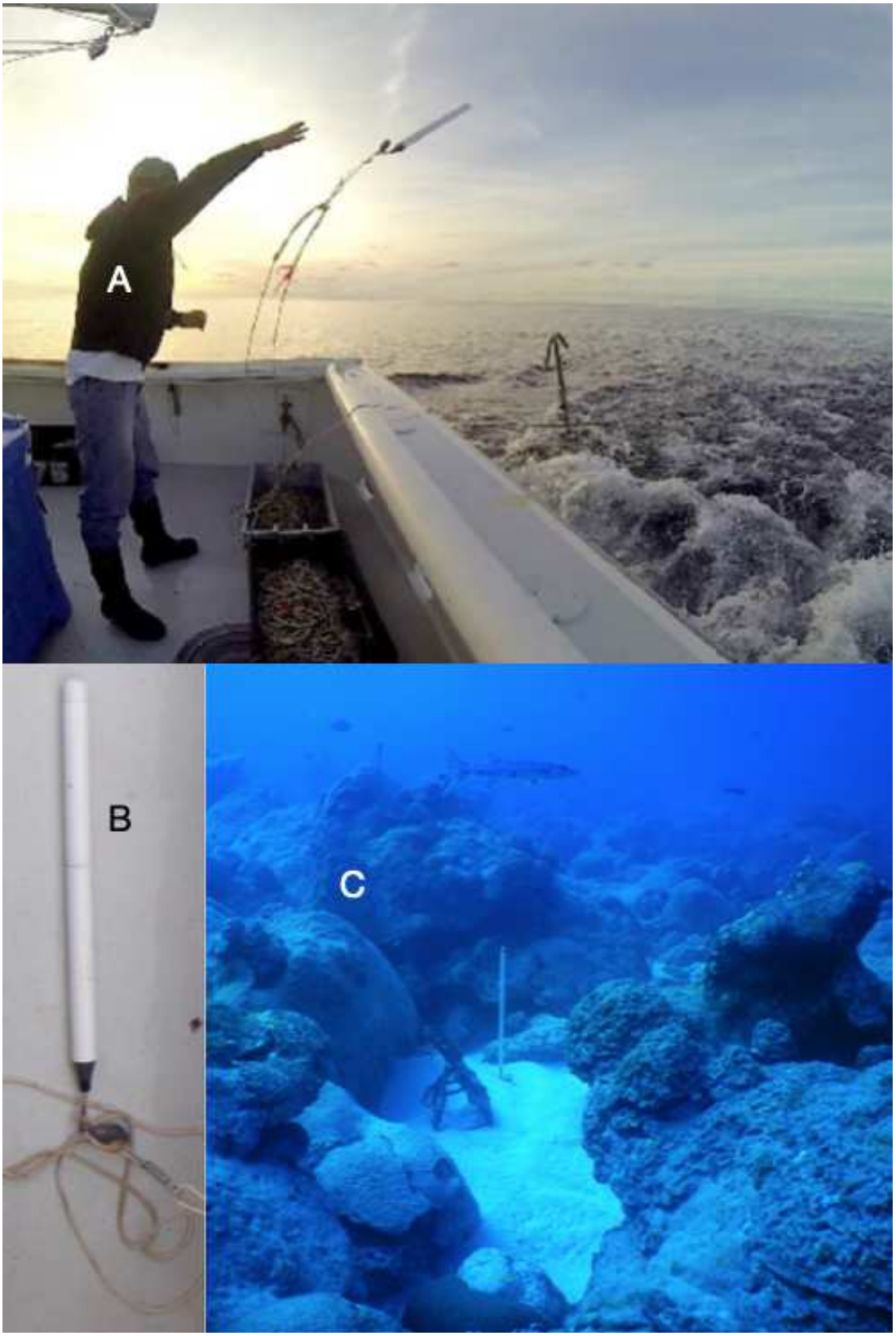

Figure 7: In the upper panel Joe has tossed over the anchor in a shallow water deployment and the first TCM has left his hand. The rest of the TCMs in the string are in the bait bucket at his feet. lower left: the SeaHorse TCM. lower right: a TCM deployed in the Flower Garden off the Texas coast.

3 Objectives

These are straight from the ONR proposal.

We anticipate using the sensor network to . . .

- document the frictional drag
  Frictional drag will be documented through direct covariance methods of Reynolds stresses using acoustic travel time current meters. Stress estimates will be obtained at 0.5 height above bottom, near the top of the log-layer, with stress estimates obtained at 2.5, 5.0 . . . m above boundary. These will be combined with time varying estimates of near-bottom stratification to assess how the stress evolves in response to that stratification and vertical structure of lower frequency currents.

- document the mixing of buoyancy
  Buoyancy mixing will be documented using direct covariance estimates of 3-D velocity and temperature, with temperature being related to buoyancy through moored CTD data obtained at lower sampling rates.

- document radiation of internal waveband momentum
  Waveband momentum radiation will be assessed using direct covariance estimates of 3-d velocity and 3-d velocity with density (for the flux of horizontal angular momentum). Attempts to relate these metrics of momentum flux with coherent features diagnosed from temperature measurements obtained from loggers placed at high density along the mooring cables.

- document radiation of internal waveband energy
  Waveband energy radiation will be documented by using the high density temperature logger data to vertically integrate the hydrostatic relation to estimate the baroclinic pressure perturbation, and then using a bottom pressure recorder placed on the mooring anchor to provide an estimate of the time varying bottom pressure in the vertical integral of the density anomaly. We will attempt to relate these metrics of energy flux with coherent features diagnosed from temperature measurements.

- document the structure of the planetary boundary layer
  The vertical of structure of velocity and density profiles on time scales longer than those characterizing the internal waveband fluxes will be estimated alongside the companion estimates of the momentum and energy fluxes.

- document the potential vorticity structure of the boundary layer
  The Ertel potential vorticity is a scalar quantity formed from 3-dimensional gradients of both velocity and density. The distributed sensor network provides very high spatial resolution from TCM strings along the boundary and very high spatial resolution from three conventional taut wire moorings in the vertical. All sensors provide data at temporal resolution in excess of 1 Hz. The high spatial resolution permits unambiguous resolution of the gradients both along and normal to the boundary and the triangular configuration of the taut wire moored array enables a projection of the densely sampled along boundary gradients onto the more sparsely sampled horizontal project of the taut wire moored array.

- document the space-time scales of coherent features *along* the boundary, 1 m from the sea bed, and the projection of these coherent features off the boundary.
  The TCM atring array represents an antenna and enables space-time coherence estimates of velocity and temperature. These quantify the prevalence and importance of phenomena such as hairpin vortices and mass ejection from the bottom boundary, time dependencies in flow separation and internal hydraulics, and can be compared with space-time scales of fastest growing submesoscale instabilities.
- document the spatio-temporal evolution of deep ocean hydraulic fronts. –JK added–
- fill in the crucial data and knowledge gaps that will be present in an interior-only observing effort.

3.1 Equations: Yummy

Placeholder here. points to make: averaging process could define turbulence and internal waves. The ambiguity is resolved by having access to inertial subrange, flux containing scales and nonlinear transports; and metrics for non-hydrostatic conditions and 3-D turbulence. Ability to distinguish wave drag from viscous drag. All this enabled by having a high resolution 3-D vertical velocity

We start from a Reynolds decomposition of the equations of motion, in which variables ϕ have been decomposed into a mean $\overline{\phi}$ and perturbation ϕ'. This act itself carries with it a certain ambiguity: The mean could represent time invariant conditions or slowly varying subinertial times scales, or even internal waveband processes. The perturbation could represent subinertial times scales, internal waves (superinertial) or 2-dimensional and or 3-dimensional turbulence. In section **??** we discuss a variety of phenomena which imply the locus of turbulent fluxes is within the internal waveband over steep and rough topography. In the following, the three-dimensional velocity is $\mathbf{u} = (u, v, w)$, ρ is density, g is gravity, f is the Coriolis parameter relating to the local pendulum day and p is pressure. A bold font is used to indicate a vector quantity. The Reynolds averaged equations are

$$\frac{\partial \overline{u}}{\partial t} + \overline{\mathbf{u}}\cdot\nabla\overline{u} + \nabla\cdot\overline{u'\mathbf{u}'} - f\overline{v} = -\frac{1}{\rho_0}\frac{\partial \overline{p}}{\partial x} \tag{1a}$$

$$\frac{\partial \overline{v}}{\partial t} + \overline{\mathbf{u}}\cdot\nabla\overline{v} + \nabla\cdot\overline{v'\mathbf{u}'} + f\overline{u} = -\frac{1}{\rho_0}\frac{\partial \overline{p}}{\partial y} \tag{1b}$$

$$\frac{\partial \overline{w}}{\partial t} + \overline{\mathbf{u}}\cdot\nabla\overline{w} + \nabla\cdot\overline{w'\mathbf{u}'} = -\frac{1}{\rho_0}\frac{\partial \overline{p}}{\partial z} - \overline{b} \tag{1c}$$

$$\frac{\partial \overline{\rho}}{\partial t} + \overline{\mathbf{u}}\cdot\nabla\overline{\rho} + \nabla\cdot\overline{\rho'\mathbf{u}'} = 0 \tag{1d}$$

in which variations of density in the momentum equations are retained only when they appear in terms multiplied by gravity g; buoyancy is $b = -g(\rho - \rho_0)/\rho_0$; and ρ_0 is a constant reference density. Equations (1) are complemented by a continuity equation, $\nabla\cdot\mathbf{u} = 0$. The direct impacts of molecular processes are assumed to be small with respect to the effects of turbulent transports: there is an inner scale of turbulent microstructure where gradient variances are dissipated by molecular processes. This scale is much smaller than the 'outer' scales that characterize the turbulent fluxes.

A common device is to describe the net effects of turbulent fluxes $\mathbf{F}_\phi$ using flux-gradient relations, which in turn has an intellectual grounding in mixing length theory. In one dimension:

$$F_\phi \equiv \overline{u'_\perp \phi'} = -K_\phi \nabla_\perp \overline{\phi} \qquad \text{flux} - \text{gradient relation} \tag{2a}$$

$$\phi' = \ell_{\text{mix}} \nabla_\perp \overline{\phi} \qquad \text{mixing length} \tag{2b}$$

in which $u'_\perp$ is normal to mean isopleths of $\overline{\phi}$, $\nabla_\perp \overline{\phi}$ is the normal gradient and ℓ_{mix} the 'mixing length'. This comes with important caveats: it is a 'local' closure relating K_ϕ to the gradient at that point. As such it is unlikely to be an accurate summary of convection set up in a downwelling Ekman layer or near boundary wave overturning relating to linear internal wave kinematics rather than dynamical instabilities, or situations in which turbulent transport terms contribute to a scalar variance budget.

3.2 Momentum

3.3 Buoyancy

3.4 Temperature Variance

The issue can be seen most clearly by considering a temperature variance equation. After invoking a Reynolds decomposition into mean and perturbation, discarding terms relating to molecular diffusion of the mean state and assuming the flow to be incompressible, one arrives at:

$$\begin{array}{ccccccc} \partial_t \overline{T'^2} & + & \overline{u} \cdot \nabla \overline{T'^2} & + & \overline{\boldsymbol{u}' T'} \cdot \boldsymbol{\nabla} \overline{\theta} & + & \boldsymbol{\nabla} \cdot \overline{\boldsymbol{u}' T'^2} \quad \cong \quad -\chi/2 \\ 1 & & 2 & & 3 & & 4 \qquad\qquad 5 \end{array} \tag{3}$$

Term 1 in (3) represents the slow time rate of change of temperature variance and term 2 a similar slow advection by the mean. Term 3 represents production of temperature variance and term 5 represents the rate of dissipation of temperature variance. Term 4 represents nonlinear cross-scale transport of temperature variance. Dimensional analysis reveals that terms 3, 4 and 5 are of similar order of magnitude. Term 4 is typically neglected by arguing that integration over a sufficiently large volume averages over spatial inhomogeneities and implies a balance between terms 3 and 5. The one-dimensional model follows suit and additionally assumes that vertical fluxes dominate in term 3, invokes a flux gradient closure (i.e. $\overline{w'T'} = -K_\theta \overline{\theta}_z$) and then rotates into a slope normal coordinate system.

3.5 Energy

Placeholder text: want to support direct estimate of $\overline{p'\mathbf{u}'}$. Want to bring up issue of nonlinear transports (triple correlations) in energy equation (or more generally, variance equation).

The second quantitative grounding for this study is an equation for the evolution of the energy spectral density, $E(\mathbf{p},\mathbf{r})$, where $\mathbf{p}$ is a three dimensional wavenumber and $\mathbf{r}$ is a representation of

a three dimensional spatial coordinate. With assumptions that linear internal wave kinematics provide a leading order description of the internal wavefield (i.e. group velocities $\mathbf{C}_g$ and polarization relations), one has

$$\frac{\partial E}{\partial t} + \nabla_{\mathbf{r}} \cdot \mathbf{C}_g E + \nabla_{\mathbf{p}} \cdot \mathscr{R} E + \mathscr{N}\mathscr{L} = S_o - S_i \tag{4}$$

where the spatial and spectral dependence is implicit. $\mathscr{R}$ represents the rate of refraction in the spectral domain, similar to the role that $\mathbf{C}_g$ plays as the rate of refraction in the spatial domain, $\mathscr{N}\mathscr{L}$ represents nonlinear transfers, S_o interior sources and S_i interior sinks. A set of boundary conditions completes the problem (see *Polzin and Lvov* (2011) for their mathematical representation). These boundary conditions could represent, for example, sourcing of an internal tide from the bottom boundary, wave reflection from a sloping boundary, wave scattering, the lateral propagation of a low-mode tide through a control volume, etc.

3.6 Potential Vorticity

The observations will be analyzed and interpreted in the dynamical framework of the flux form of the PV equation (*Marshall and Nurser*, 1992), i.e.

$$\partial q/\partial t + \nabla \cdot \mathbf{J} = \mathbf{0} \ . \tag{5}$$

Here, $q = \omega_a \cdot \nabla b$ is the potential vorticity (PV), $\omega_a = f\mathbf{k} + \nabla \times \mathbf{u}$ the absolute vorticity, f the Coriolis parameter, $\mathbf{u}$ the 3-d velocity, b buoyancy, and stratification N^2 is the vertical gradient of b. The PV flux is $\mathbf{J} = \mathbf{u}q + \nabla b \times \mathbf{F} - \omega_{\mathbf{a}} D$. Equation (5) states that the time rate of change of PV within a control volume is determined by the convergence of advective ($\mathbf{u}q$), frictional ($\nabla \mathbf{b} \times \mathbf{F}$) and diabatic ($\omega_{\mathbf{a}} D$) components of the PV flux, where $\mathbf{F}$ is the frictional force (e.g., by bottom stress or bluff form drag) and D is the rate of change of buoyancy due to diabatic processes (i.e., diapycnal mixing). Demonstration of the framework's effectiveness and insight potential is provided by the PycnoGen team's proof-of-concept application in the North Atlantic (*Thompson et al.*, 2016; *Yu et al.*, 2019).

The fundamental questions this white paper addresses concern the relative roles of gravity and rotation in modifying potential vorticity in the ocean's bottom boundary layer. There is a wealth of understanding about the relative roles in the ocean's surface boundary layer, in which the dichotomy can be drawn as a shear instability and direct convection vs mixed layer baroclinic instabilities (*Boccaletti et al.*, 2007) and forcing that produces anamolously signed potential vorticity, which in turn projects upon submesoscale instabilities (*Thomas et al.*, 2008). At the ocean's bottom boundary, isopycnals intersect sloping topography and thus the coupling of the interior with the kinematic condition of no flow through the bottom can project the dynamical boundary conditions on momentum and buoyancy in a much different fashion. The superposition of small scale topography upon an inclined slope emphasises this difference: Gravity acts on a fast time scale, rotation acts on a slow time scale and small spatial scales inherent in complex topography emphasize short time scales. These small spatial scales can combine with external forcing on fast time scales (i.e. tides and an ambient internal wavefield) such that the development of bottom boundary layer closure schemes for a hierarchy of numerical models becomes a very nuanced proposition.

We prioritize the issue of potential vorticity as the slow time evolution of a fluid parcel in the presence of rotation is controlled by the distribution of potential vorticity (*Pedlosky*, 2013). The distribution of potential vorticity dictates low frequency ocean flows, what instabilities are present and how wave/tides propagate throughout the water column. The distribution of potential vorticity

in the ocean interior is controlled by mixing across isopycnals and torques applied at the ocean boundaries (*Haynes and McIntyre*, 1987).

Potential vorticity can be concieved as a material property of a fluid parcel, so that one paradigm for potential vorticity modification is to consider a turbulent model that focusses upon the water parcel, i.e. viscous or bluff form drag at the bottom , the development of mixed layers, the ejection of mass from the boundary by hairpin vortices or internal bores, and flow separation and/or internal hydraulic transitions as water parcels navigate around or over finite amplitude topography. This is not the only vehicle for potential vorticity modification as torques can come in association with an internal wave momentum flux divergence with the internal wave momentum flux being a property of wave generation at the boundary. Ultimately, this boundary forcing projects projects onto a non-orthogonal space of gravity, topographic and planetary waves (*Rhines*, 1970) to impact global system behavior.

4 Science Objectives / Sensor Network Goals

There is a preface here that touches on the current generation of high resolution numerical models to support regional recirculations associated with PV injection associated with flow separation from headlands - California Current, GoM, Rockall Trough ....

4.1 Boundary Currents and Ekman Layers

Currents along sloping topography that are in the direction Kelvin wave propagation - shallow topography on the right when facing with the current in the northern hemisphere - are associated with downslope Ekman transports. These downslope transports advect light water under dense, creating convectively unstable conditions. The combination of frictional torques and mixing of buoyancy that is a consequence of convection result in the destruction of potential vorticity (*Benthuysen and Thomas*, 2012). Similarly, retrograde currents are associated with upslope Ekman transport that results in increased stratification. In this case, the boundary presents itself as a source of potential vorticity.

This issue is fundamental and our ignorance is profound. If the processes that ventilate the boundary in downwelling favorable conditions are not fast enough, the potential vorticity distribution will have a sign reversal. Free shear flows with such anomalously signed potential vorticity distributions are understood to be unconditionally unstable on time scales similar to the planetary rotation rate (*Ooyama*, 1966; *Hoskins*, 1974). However, these compete with intrinsic gravity modes associated with external forcing on that fast time scale and can be disrupted by topographic roughness that provides forcing that does not project upon the fastest growing instabilities (*Wenegrat and Thomas*, 2020).

Open Questions

- what is the nature of the instability just described? Two distinct limiting paradigms emerge: that of stratified turbulence, in which turbulent motions along isopycnals are independent of those along other isopycnals, with coupling between isopycnals limited to the height scales of vertical overturns; and that of a radiating internal waveband response.

- what is the role of boundary conditions, particularly those associated with departures from a planar slope, in determining the structure of the boundary layer and the far-field response?
- What is the nature of the processes that lead to the rapid ventilation of the boundary layer and maintenance of near-boundary stratification? Can this be related to frictional drag on the ebb phase of time dependent motions, which holds up dense water and allows lighter water to differentially advect above (*Slinn and Riley*, 1998)? Or is the ejection of mass into the stratified interior (*Winters*, 2015) fundamental?
- what is the role of external forcing (i.e. an ambient internal wavefield or barotropic tides)?
- how do time-dependent rotating hydraulics influence all of the above?

While these open questions are focused on boundary layer processes, we note that they address the forcings which directly influence the interior water column. Hence, they are or crucial importance to the interpretation, understanding, and prediction of interior water column motions.

4.2 Abyssal upwelling

The MAVS have most recently been deployed as part of the Bottom Boundary Layer Turbulence and Abyssal Recipes field program (*Polzin et al.*, 2022), with the goal of resolving fundamental questions concerning global ocean upwelling articulated in *Ferrari et al.* (2016): that upwelling in the ocean's bottom boundary layer results from small buoyancy fluxes in a weakly stratified near-bottom layer, and enhanced buoyancy fluxes in a 'stratified mixing layer'. What we found was completely different. The boundary layer was strongly stratified to within several meters of the bottom, and the underpinning assumption of downgradient fluxes (*Polzin and McDougal*, 2021) (i.e. negatively signed temperature fluxes) was contradicted by the measurements (Fig. 8). When interpreted through the lense of a diapycnal advection / diffusion balance (*McDougall*, 1989), the observed temperature flux estimates predict a substantial (100 m / day) diapycnal velocity that is consistent with observations from an intentional dye release.

4.2.1 Conceptual Models

Our current understanding of the Ocean Bottom Boundary Layer (OBBL) is encapsulated by what is referred to as the 'one-dimensional model'. We point the reviewer to an extensive review in *Polzin and McDougall* (2022).

The one-dimensional model has two fundamental assumptions: First, that the fluxes giving rise to turbulent production are dominated by those aligned with gravity, and second, that these turbulent fluxes can be characterized by a flux-gradient relation, i.e. a mixing length closure that discards transport terms associated with triple correlations. This model makes several fundamental predictions: that the near-boundary region is weakly stratified relative to the interior and that buoyancy fluxes have a mid-depth minimum, with diapycnal upwelling hard up against the boundary and diapycnal downwelling in the highly stratified turbulent interior.

A growing body of evidence suggests that neither of these predictions enjoys observational support over steep and rough, i.e. complex, topography (*Polzin et al.*, 2021, 2022; *van Haren et al.*, see also figure 8). Key insights from these observations are that horizontal fluxes giving rise to turbulent production are often far larger than those in the vertical, consistent with the basic physics underlying adiabatic internal waveband motions and that differential advection of buoyancy associated with internal wave band motions is inconsistent with a flux-gradient closure. In short,

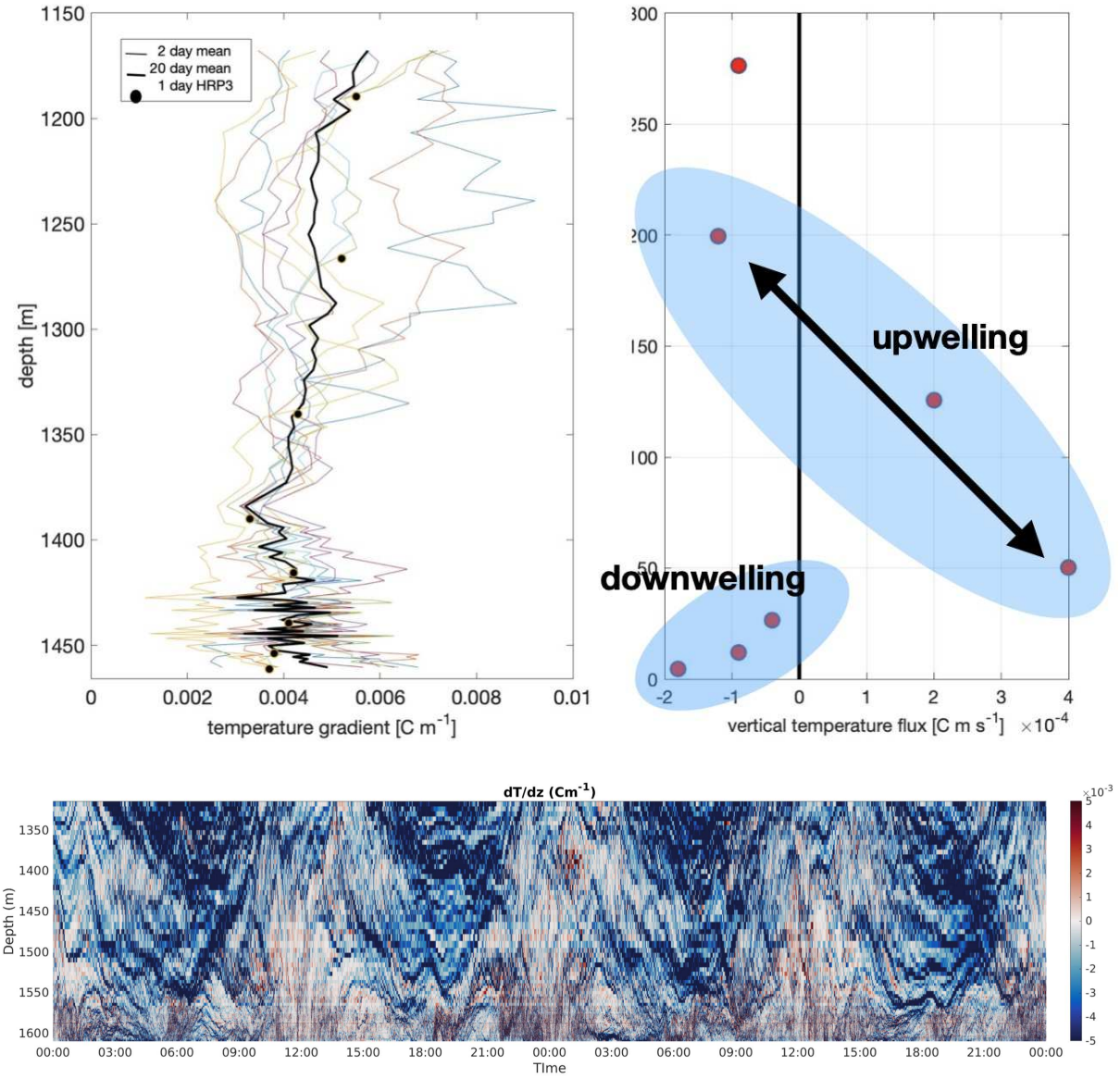

Figure 8: Moored temperature and current meter data from a mooring placed along the axis of a steep-sided canyon in the Rockall Trough *Polzin et al.* (2022). A total of 80 temperature recorders were placed on this 300 m tall mooring along with 8 MAVS current meters and a downward looking ADCP. Record lengths of 72 days provide robust statistics in which the essential patterns of the temperature flux emerge within a fortnight. Left hand panel: The temperature data reveal that the water column is well stratified in the mean on time scales of several days, with no indication of a well mixed near-boundary region at 20 days average.
Right hand panel: vertical profile of moored temperature flux from MAVS. With little to no vertical trend in temperature gradients, mean isotherms are nearly horizontal. Thus, from a diapycnal advection - diffusion balance, increasing vertical temperature fluxes with increasing height above bottom indicate downwelling and decreasing trends indicate upwelling across mean isopycnals. Estimates of terms in a temperature variance budget indicate that the positive values of the temperature flux are balanced by the divergence of triple correlation terms, so that the leading order balance is non-local, as one might expect from a wave breaking process.
Bottom panel: a time-depth series of temperature gradient from the moored temperature recorder data. The time series is two days long and one finds evidence for a episodic wave breaking process having semi- diurnal periodicity at mid-water column that supports the interpretation of a highly non-local process. Figure courtesy of Carl Spingys.

the one-dimensional model exhibits many of the characteristics of a body of literature known as 'Fairy Tales', as alluded to in the Introduction of *Polzin and McDougall* (2022). Such a realization is crucially important to our ability to understand, interpret and predict interior water column processes.

The buoyancy anomaly of the one-dimensional model has attracted growing interest as an extension of closures for mixed layer baroclinic instabilities and submesoscale instabilities in the Ocean Surface Boundary Layer. At the largest scales, reversal in the sign of the potential vorticity gradient can give rise to topographically modified submesoscale baroclinic instabilities (*Wenegrat et al.*, 2018; *Callies*, 2018). A more significant buoyancy anomaly in the one-dimensional model can be associated with anomalously signed potential vorticity, giving rise to submesoscale instabilities (*Allen and Newberger*, 1998; *Wenegrat and Thomas*, 2020). These concepts and closures might elucidate the behavior climate models, but are completely inappropriate for prediction of the BattleSpace environment where fidelity to the physical environment rather than abstract theories are valued.

4.3 The Nature of "Friction" and its Impact on Global System Behavior

It is a fundamental tenet of the partial differential equations governing geophysical fluid dynamics that the interior solution is strongly controlled by the boundary conditions. These boundary conditions are communicated through planetary wave dynamics to control global system behavior. While it is reasonable to neglect to ocean bottom boundary layer when studying upper ocean dynamics, this is only half the problem that determines global system behavior.

The linkage between boundary conditions and planetary wave dynamics is the aegis for western boundary currents articulated in *Stommel* (1948) and *Munk* (1950): Western Boundary Currents are on the western boundary due to friction. These results are essentially about the properties of mathematical operators and have absolutely NOTHING to do with observations of boundary mixing.

> Barotropic models are idealized in that they represent horizontal pressure gradients along vertical sidewalls as a delta function. With stratification and finite topographic slopes baroclinic pressure gradients along sloping topography can play a similar role (*Hughes and De Cuevas*, 2001) as the frictional operators. Consideration of JEBAR.

However, we find *Sheremet et al.* (2022) arguing that, within a certain part of parameter space, friction is essential to determining the three stationary states the Loop Current. Transitions between such hypothetical stationary states are excruciatingly difficult to predict numerically - Joe. It is a simple process to concoct a hypothesis that the numerical models are simply not in the proper parameter space because of their bottom boundary. closure schemes and topographic filtering. Understanding the importance of friction in a more general context of flow-topography interactions and a mapping of that boundary forcing into the interior provides a pathway to rationalizing why subtle changes in the representation of small scale topography in numerical models can alter the path of major currents such as the Antarctic Circumpolar Current (*Zhang and Nikurashin*, 2020) and the Gulf Stream (*Chassignet et al.*, 2023) as well as underpinning state transitions.

More generally we can ask: How are flow topography interactions communicated via planetary wave dynamics to impact global system behavior such as the meridional overturning in the Southern Ocean and it vertical structure, and to synthesize elements involving the production and dissipation of thermohaline variability that are symptomatic of cross-frontal transport.

4.4 Cross-Shelf transports, Gravity Currents and Bottom Water Production

Sometime in the not too distant future a newly conceived water parcel, made cold and dense by exposure to cryogenic processes, will teeter at the edge of a shelf break, teetering, and then fall into the abyss. As it does so it will be given the directive, "Go West, Young Water".

Truth be told, this has been going on since time immemorial: It is the *beginning* of the story of an abyssal boundary current, the one which describes the transformation of the watermass from its journey at the shelf break to its arrival in the abyss rather than the story penned in Stommel and Arons (1962) about how that water parcel wanders the globe in search of warmth and light through the process of upwelling (Munk 1966).

This initial chapter is also a story that has been told before, in particular from the perspective of layered gravity current dynamics (Legg) in which a barrier exists between the fluid at the boundary and the rest of the boundary current, thereby limiting communication of the boundary conditions with the rest of the boundary current. The intent here is to describe the gravity current paradigm from the perspective of a continuously stratified fluid. Whether the distinction between layered or continuous perspectives leads to different behaviors is unclear at this time and an objective of our study. Time dependence is likely a key issue, where gravity currents propagate (cascade?) down slope akin to roll waves and avoid the development of well mixed bottom layers.
The westward imperative is understood as a simple consequence of westward planetary wave propagation translated onto a sloping boundary. This westward propagation combines with bottom drag to produce a downwelling Ekman layer, one in which the boundary is a sink for potential vorticity and capable of producing conditions of anomalously signed potential vorticity that are unconditionally unstable at frequencies of f.

It is time to study this problem. It is abetted by advancements in technology that permit resolution of turbulence and mixing from conventional moorings.

4.5 Carbon and Terraforming

Boundary mixing on the Continental Slope plausibly impacts the Carbon budget in two ways.

(1) There is an 'intake phase'. The upwelling of nutrients and oxygen up the Continental Slope and onto the Continental Shelf represents inputs at the base of the food chain. Once in the euphotic zone, increased nutrients provide fuel for phytoplankton, which are grazed on by zooplankton, upward and onward to charismatic macrophauna. There is an issue here, in that while deep water tends to be nutrient rich, it is also rich in dissolved CO2, which degasses with decreasing pressure. There needs to be a fairly detailed, quantitative budget that asks whether / how providing increased nutrients might actually result in increased natural carbon sequestration.

(2) There is an exhaust phase. If you can fluidize carbon rich sediments on the Continental Shelf, there is the potential to export across the shelf and into the deep ocean.

Into (1) and (2) we ask, do we understand enough about the fluid dynamics of cross-slope transport aka boundary mixing to terraform the slope to either enhance / reduce fluxes of carbon relevant variables. For instance, can we chanalize the shelf break to sequester fluidized sediment to greater depth. In this, there is a calculation: the carbon credit industry in ten years is projected at 30 Billion dollars per year, and thus for every meter of depth horizon that one can push sediment there is an increased time scale and a dollar sign. A small fraction of $30 Billion is a large number.

Hence: do we understand the physical dynamics of internal hydraulics well enough to rent a very large vessel with a very large pump to engage in the equivalant of hydraulic mining on the Continental Slope?

5 Numerical Modeling

5.1 The Closure Issue

Numerical models are budget keeping devices that are a necessary evil in the context of ocean state prediction. We rely upon them to project boundary forcing into the interior and into the future. They have significant limitations, though, as much of that forcing is really nasty nonlinear shit that does not map nicely into either our preconceived notions of ocean behavior or the numerical grids. We discuss this with the point that reliance conceptual models of how the ocean ought to behave without the process of empirical ratification is . . . well, it isn't Science.

5.1.1 Basic Limitations of Numerical Models

For the scope of this discussion there are three key elements in the energy balance for the internal wavefield. We illustrate these using an example from the Brazil Basin.

The first element is that models of oscillatory flow over sloping topography, e.g. tides, prescribe the energy density of the radiated internal wave (tide) as being proportional to the topographic slope density. The regional root-mean-square (rms) topographic slope in the Brazil Basin is dominated by 'abyssal hills' having a distance between peaks of 6-8 kilometers and rms heights of approximately 150 m. These lead to conditions that are approximately critical with regards to semi-diurnal internal tide trajectories. As a result, strong, bottom enhanced turbulence is anticipated above such hills. This is quantitatively addressed in *Polzin* (2004b) using analytic solutions to a radiation balance equation with non-linear transfers rescribed by a spectrally *local* representation of the heuristic diagnostic know as the Finescale Parameterization *Polzin* (2004a). The agreement between observations and prediction is remarkable and improves when scattering is included. The magnitude and decay scale directly relates to a peak in the internal wave shear spectrum at 120 m vertical wavelength and 1000 m horizontal wavelength. Using a numerical model to simulate the processes at play raises an obvious issue:

> A numerical model with increasingly coarser resolution than that required to represent a 1 km horizontal wavelength will not be able to quantitatively describe both generation and scattering and, as a result of diminishing the effects of scattering, will over-emphasize the ability of larger scale tides to propagate.

The second key element concerns the character of the nonlinear interactions. The Finescale Parameterization implicitly assumes that energy transfers in horizontal wavenumber keep pace with those in vertical wavenumber so that, as energy is transferred to smaller vertical scales, there is no significant change in wave frequency. The Finescale Parameterization is heuristic, i.e. empirically grounded with minimal theoretical under-pinning. The theoretical description of internal wave interactions of 3 decades ago (*Müller et al.*, 1986) emphasized extreme scale interactions, and in

particular the role of high frequency internal wave refraction in near-inertial shear along a phase velocity equals group velocity resonance. This characteristic interaction is not manifested in diagnostic analyses of data (*Sun and Pinkel*, 2012). *Lvov and Polzin* (2023) and *Polzin and Lvov* (2023) provide a rigorous theoretical assessment of this interaction. In Eulerian coordinates, this interaction has the shortest time scale and is thus the most important driver of nonlinearity. However, it shares this short timescale with a Bragg scattering process. Viewed from a ray-characteristic coordinate system (a Lagrangian perspective), the Bragg scattering process eliminates the anisotropic conditions that are behind the energy exchanges of the phase velocity equals group velocity resonance. The end result of such subtractive cancellation is an emphasis on the next fastest timescale, that characterizing local interactions embodied in the Finescale Parameterization (*Dematteis and Lvov*, 2021; *Dematteis et al.*, accepted). The implication for realistic prediction model is that:

> A numerical model that uses a stretched grid, i.e. one in which the horizontal grid is longer than the vertical grid is tall, will diminish and possibly eliminate this Finescale pathway for energy transfers. The consequences for model behavior are unclear.

The third model deficiency is the translation of bottom topography into bottom boundary conditions. The fully resolved topography in the Brazil Basin example is finite amplitude in that ray trajectories are similar to the topographic slope (*Polzin*, 2004b, 2009). This, in turn, implies issues of flow block and internal hydraulics or flow separation and similar nasty nonlinear phenomena. The mathematical treatment of finite amplitude topography is that the no-flow boundary condition is placed at the bottom boundary and is thus nonlinear in topographic height. In contrast, a linear model will specify the corresponding vertical velocity along a plane of uniform depth. In relation to ocean models,

> the simple act of filtering topography in acknowledgement of limited numerical resolution or numerical stability criteria is in fact a linearization of the problem that can eliminate basic phenomena.

This brings us to a fourth issue.

Topography is routinely filtered to explicitly reduced the topographic slope for reasons of numerical stability. The issue appears to be that of extrapolating the pressure to grid center. Per Alister Adcroft, the MIT GCM appears to be the best of the lot with a partial cell formulation. ROMS: 1/9? topographic slope.

Due to topographic filtering and numerical resolution that limits internal wave variability, the present generation of global models is unable to realistically represent the internal wave driven mixing that underpins global ocean upwelling. Instead, mixing is explicitly prescribed (*MacKinnon et al.*, 2017; *Mashayek et al.*, 2017) with disparate notions about the treatment of topographic variability in control volume budgets (*Polzin*, 2009; *McDougall and Ferrari*, 2018) and *ad hoc.* treatments of mixing suppression (*Ferrari et al.*, 2016) at the boundary. The disparate opinions are covered extensively in *Polzin and McDougal* (2021).

A naive take would be to suggest that since plane internal waves have no perturbation potential vorticity signature, that underestimating the internal wave climatology will present no consequences for the long time scale behavior of the model. The premise about plane wave formulations is off point: A plane Rossby wave also has no perturbation potential vorticity signature. The issue is that both internal wave and Rossby wave *packets* have a perturbation potential vorticity signature associated with the momentum flux divergence of the packet structure, e.g. *Bühler and McIntyre* (2005) With this packet structure comes the potential for stirring potential vorticity through a combination of internal wave - mean flow and internal wave - internal wave nonlinear interactions (*Polzin*, 2010; *Polzin and Lvov*, 2011).

This act of filtering will have strong implications for the production of PV anomalies associated with internal hydraulic transitions and flow separation.

In summary, we can not trust numerical model results to represent these bottom boundary layer processes and hence their influence on interior water column dynamics. Thus, the success of an interior water column observing effort will hinge directly on observations of the bottom boundary layer.

5.1.2 Standard Closures, KPP as the best of the lot

KPP is just the OSBL turned upside down, with no representation of the internal wave-band processes that are responsible for restratification (maintaining a stratified near-boundary region)

6 Benediction

There is a knowledge gap concerning the structure and behavior of the ocean's bottom boundary layer that keeps us from .... Inaction on this issue is aided and abetted by the lack of observational ground truth to point out a better way forward. To our knowledge, the only system which can fill this gap in knowledge is our Distributed Sensor Network. The Distributed Sensor Network is proven technology having evolved over 5 decades of development. What is unique in this application is the insight that network assets can be deployed to assess the issue of potential vorticity modification at the ocean's bottom boundary. We propose to obtain estimates of energy, momentum and potential vorticity fluxes using direct covariance methods and relate these to the structure and phenomenology of the bottom boundary layer. The nature of this effort is transformative rather than incremental.

A Window on the Future
The business model that permits sourcing one sensor network per year over a decade is less than $10M US per year. The scoping depends upon how one counts engineering solutions, seagoing resources, initial data analysis and preliminary numerical support. Current NSF resources to support such an effort are inadequate. The only way forward is through a community level program. This is an international community such as that envisioned with venues such as the Gordon Research Conference on Ocean Mixing. In response to program managers who would suggest that the ask is too great, our response is, "Your budget is too little. Let us help you get more."

7 Appendix: Engineering Challenges and Solutions

A standard MAVS-5 produced by Nobska Development Corporation is configured to return either four path velocities or 3-axis velocity in instrument or geographic frames, and instrument tilts and tilt-corrected magnetometer data for the instrument heading. This standard instrument has the following limitations.

- Sampling rates of ≤ 5 Hz are limited by the time required to interrogate the compass.
- The standard MAVS-5 has an 18 A-hr internal Lithium battery pack, limiting total data acquisition.
- The tilt sensor cannot differentiate between tilts or horizontal acceleration.
- The instrument is run by a Persistor (CF2) controller having a 4 GB SD card limit for data storage.
- The Persistor was last manufactured in 2007, and funding this grant would exhaust Nobska's stock.

The PI has been testing and deploying the MAVS current meters on conventional taut wire moorings for the past seven years (*Polzin et al.* (2021), *Naveira Garabato et al.* (2019) - see Figure 2). This platform presents a more challenging sampling environment for turbulence and turbulent flux measurements than either a bottom lander or a float, due to the potential for vortex-induced vibrations to result in package motion and contaminate the velocity measurements. To date, such vortex-induced vibrations have not limited the data analysis: if present, the contamination simply needs to be acknowledged and avoided in the data processing through appropriate filtering. We have been diagnosing this issue by placing MAT-1 accelerometers / magnetometers manufactured by Lowell Engineering in association with the current meters, and sampling those sensors at 64 Hz. These data provide the following insight: the basic issue is consistent with strumming from a 3/16-inch mooring cable that projects onto a Strouhal frequency of 6-8 Hz. which becomes noticeable at flow speeds of approximately 20 cm s^{-1}. The MAV's maximum sampling rate of 5 Hz aliases this. A secondary issue is that, at flow speeds of 30-40 cm s^{-1}, a torsional motion develops having a period of approximately 1 minute. This is likely associated with the upper spherical flotation rotating through $\pm 180^{\circ}$. The current combination of tilt sensors and tilt-corrected compass provides for some, but not all, of the required correction.

Extensive experience deploying these sensors on conventional moorings (*Polzin et al.*, 2021; *Naveira Garabato et al.*, 2019) (Fig. 2) has led to a program of performance enhancements in collaboration with Nobska Development Corporation and T2 Embedded Systems. To date we have, (i) a 500 A-hr external battery pack power solution, (ii) provided power conditioning to limit battery degradation at low temperature resulting from pulsatile current requests; and (iii)

eliminated time base issues in temperature flux measurements by logging serial data from a custom RBRcoda^3 T temperature probe (Fig. 2), whose tip is placed into the measurement volume of the current meter. We have also built and tested a custom current meter with a VN-100 motion package. Logging of the 3-axis magnetometer and accelerometer data permit post-processing to remove artifacts relating to package motion. Turning off the standard compass and tilt sensor permits logging by the CF2 at substantially higher rates. Recent funding of an NSF proposal (OCE-2232439, The Internal Wave Spectrum and Boundary Mixing in the Sub-Tropical South Atlantic) will advance this effort by having path velocities, VN-100 and RBR data logged by a Teensy micro-controller onto a micro-SD card. The combination of daisy-chaining two battery packs, increased storage on a micro-SD card, and sensor upgrades, will permit us to sample the MAVS at 10 Hz for one year, and will result in enhanced signal-to-noise levels. In this incarnation, the CF2 is still required for its low-level programming that controls the travel time circuitry. This brings about an additional complication: we will have used up the remaining inventory of CF2 micro-controllers.

References

Allen, J., and P. Newberger (1998), On symmetric instabilities in oceanic bottom boundary layers, *Journal of Physical Oceanography*, *28*(6), 1131–1151.

Aretxabaleta, A. L., B. Butman, R. P. Signell, P. S. Dalyander, C. R. Sherwood, V. A. Sheremet, and D. J. McGillicuddy Jr (2014), Near-bottom circulation and dispersion of sediment containing alexandrium fundyense cysts in the gulf of maine during 2010–2011, *Deep Sea Research Part II: Topical Studies in Oceanography*, *103*, 96–111.

Benthuysen, J., and L. N. Thomas (2012), Friction and diapycnal mixing at a slope: Boundary control of potential vorticity, *Journal of Physical Oceanography*, *42*(9), 1509–1523.

Boccaletti, G., R. Ferrari, and B. Fox-Kemper (2007), Mixed layer instabilities and restratification, *Journal of Physical Oceanography*, *37*(9), 2228–2250.

Bühler, O., and M. E. McIntyre (2005), Wave capture and wave–vortex duality, *Journal of Fluid Mechanics*, *534*, 67–95.

Callies, J. (2018), Restratification of abyssal mixing layers by submesoscale baroclinic eddies, *Journal of Physical Oceanography*, *48*(9), 1995–2010.

Cane, M. A., V. M. Kamenkovich, and A. Krupitsky (1998), On the utility and disutility of jebar, *Journal of Physical Oceanography*, *28*(3), 519–526.

Chassignet, E. P., X. Xu, A. Bozec, and T. Uchida (2023), Impact of the new england seamount chain on gulf stream pathway and variability, *Journal of Physical Oceanography*.

Cole, S. T., J. M. Toole, R. Lele, M.-L. Timmermans, S. G. Gallaher, T. P. Stanton, W. J. Shaw, B. Hwang, T. Maksym, J. P. Wilkinson, and M. Ortiz (2017), Ice and ocean velocity in the arctic marginal ice zone: Ice roughness and momentum transfer, *Elementa: Science of the Anthropocene*, *5*.

Davis, P. E., and K. W. Nicholls (2019), Turbulence observations beneath larsen c ice shelf, antarctica, *Journal of Geophysical Research: Oceans*, *124*(8), 5529–5550.

Dematteis, G., and Y. V. Lvov (2021), Downscale energy fluxes in scale-invariant oceanic internal wave turbulence, *Journal of Fluid Mechanics*, *915*.

Dematteis, G., K. L. Polzin, and Y. V. Lvov (accepted), On the origins of the oceanic ultraviolet catastrophe, *Journal of Physical Oceanography*, *52*.

Ferrari, R., A. Mashayek, T. J. McDougall, M. Nikurashin, and J.-M. Campin (2016), Turning ocean mixing upside down, *Journal of Physical Oceanography*, *46*(7), 2239–2261.

Haynes, P. H., and M. E. McIntyre (1987), On the evolution of vorticity and potential vorticity in the presence of diabatic heating and frictional or other forces, *Journal of Atmospheric Sciences*, *44*(5), 828–841.

Holloway, G., and P. Rhines (1991), Angular momenta of modeled ocean gyres, *Journal of Geophysical Research: Oceans*, *96*(C1), 843–846.

Hoskins, B. (1974), The role of potential vorticity in symmetric stability and instability, *Quarterly Journal of the Royal Meteorological Society*, *100*(425), 480–482.

Hughes, C. W., and B. A. De Cuevas (2001), Why western boundary currents in realistic oceans are inviscid: A link between form stress and bottom pressure torques, *Journal of Physical Oceanography*, *31*(10), 2871–2885.

Ierley, G. R. (1990), Boundary layers in the general ocean circulation, *Annual review of fluid mechanics*, *22*(1), 111–140.

Ierley, G. R., and V. A. Sheremet (1995), Multiple solutions and advection-dominated flows in the wind-driven circulation. part i: Slip, *Journal of marine research*, *53*(5), 703–737.

Kunze, E., A. J. Williams, and M. G. Briscoe (1990), Interpreting shear and strain finestructure from a neutrally buoyant float, *Journal of Geophysical Research*, *95*, 18,111–18,126.

Lvov, Y. V., and K. L. Polzin (2023), Generalized transport characterizations for short oceanic internal waves in a sea of long waves, *arXiv preprint arXiv:2203.03784v3*.

MacKinnon, J. A., Z. Zhao, C. B. Whalen, A. F. Waterhouse, D. S. Trossman, O. M. Sun, L. C. St. Laurent, H. L. Simmons, K. Polzin, R. Pinkel, et al. (2017), Climate process team on internal wave–driven ocean mixing, *Bulletin of the American Meteorological Society*, *98*(11), 2429–2454.

Marshall, J. C., and A. G. Nurser (1992), Fluid dynamics of oceanic thermocline ventilation, *Journal of physical oceanography*, *22*(6), 583–595.

Mashayek, A., C. P. Caulfield, and W. R. Peltier (2017), Role of overturns in optimal mixing in stratified mixing layers, *Journal of Fluid Mechanics*, *826*, 522?552, doi:10.1017/jfm.2017.374.

McDougall, T. J. (1989), Dianeutral advection, in *Parameterization of Small-Scale Processes: Proc.'Aha Huliko 'a Hawaiian Winter Workshop*, pp. 289–315.

McDougall, T. J., and R. Ferrari (2018), Reply to "comment on 'abyssal upwelling and downwelling driven by near-boundary mixing'", *Journal of Physical Oceanography*, *48*(3), 749–753.

Müller, P., G. Holloway, F. Henyey, and N. Pomphrey (1986), Nonlinear interactions among internal gravity waves, *Reviews of Geophysics*, *24*(3), 493–536.

Munk, W. H. (1950), On the wind-driven ocean circulation, *Journal of Atmospheric Sciences*, *7*(2), 80–93.

Naveira Garabato, A. C., E. E. Frajka-Williams, C. P. Spingys, S. Legg, K. L. Polzin, A. Forryan, E. P. Abrahamsen, C. E. Buckingham, S. M. Griffies, S. D. McPhail, K. W. Nicholls, L. N. Thomas, and M. P. Meredith (2019), Rapid mixing and exchange of deep-ocean waters in an abyssal boundary current, *Proceedings of the National Academy of Sciences*, *116*(27), 13,233–13,238, doi:10.1073/pnas.1904087116.

Ooyama, K. (1966), On the stability of the baroclinic circular vortex: A sufficient criterion for instability, *Journal of Atmospheric Sciences*, *23*(1), 43–53.

Pedlosky, J. (2013), *Geophysical fluid dynamics*, Springer Science & Business Media.

Polzin, K., M. Alford, G. Voet, N. Couto, A. Le Boyer, H. Allbrook, H. Drake, B. Fernandez-Castro, A. Forryan, E. Frajka-Williams, J. Hughes, C. Kermabon, Y. Kostov, H. Mercier, M.-J. Messias, A. Naveira Garabato, K. Polzin, K. Reddy, N. Ross, X. Ruan, C. Spingys, B. Wynne-Cattanach, and R. Ferrari (2022), Eddy covariance estimates of temperature and momentum fluxes from standard moorings during the boundary layer turbulence - recipes field program, ocean Sciences Meeting 2022.

Polzin, K. L. (2004a), A heuristic description of internal wave dynamics, *Journal of Physical Oceanography*, *34*, 214–230.

Polzin, K. L. (2004b), Idealized solutions for the energy balance of the finescale internal wavefield, *Journal of Physical Oceanography*, *34*, 231–246.

Polzin, K. L. (2009), An abyssal recipe, *Ocean Modelling*, *30*, 298–309.

Polzin, K. L. (2010), Mesoscale eddy–internal wave coupling. part ii: Energetics and results from polymode, *Journal of physical oceanography*, *40*(4), 789–801.

Polzin, K. L., and Y. L. Lvov (2011), Toward regional characterizations of the oceanic internal wavefield, *Reviews of Geophysics*, *49*, doi:10.1029/2010RG000329.

Polzin, K. L., and Y. V. Lvov (2023), A one-dimensional model for investigating scale-separated approaches to the interaction of oceanic internal waves, *arXiv preprint arXiv:2204.00069v2*.

Polzin, K. L., and T. McDougal (2021), Mixing at the ocean's bottom boundary, in *Ocean Mixing*, edited by M. Meredith and A. Naveira Garabato, Elsevier.

Polzin, K. L., and T. J. McDougall (2022), Mixing at the ocean's bottom boundary, in *Ocean Mixing*, pp. 145–180, Elsevier.

Polzin, K. L., B. Wang, Z. Wang, F. Thwaites, and A. J. Williams (2021), Moored flux and dissipation estimates from the northern deepwater gulf of mexico, *Fluids*, *6*(7), 237.

Ponte, R. M., and R. D. Rosen (1994), Oceanic angular momentum and torques in a general circulation model, *Journal of physical oceanography*, *24*(9), 1966–1977.

Rhines, P. (1970), Edge-, bottom-, and rossby waves in a rotating stratified fluid, *Geophysical and Astrophysical Fluid Dynamics*, *1*(3-4), 273–302.

Shaw, W. J., J. H. Trowbridge, and A. J. Williams III (2001), Budgets of turbulent kinetic energy and scalar variance in the continental shelf bottom boundary layer, *Journal of Geophysical Research: Oceans*, *106*(C5), 9551–9564, doi:10.1029/2000JC000240.

Sheremet, V. A., A. A. Khan, and J. Kuehl (2022), Multiple equilibrium states of the gulf of mexico loop current, *Ocean Dynamics*, *72*(11-12), 731–740.

Slinn, D. N., and J. Riley (1998), Turbulent dynamics of a critically reflecting internal gravity wave, *Theoretical and computational fluid dynamics*, *11*(3), 281–303.

Stommel, H. (1948), The westward intensification of wind-driven ocean currents, *Eos, Transactions American Geophysical Union*, *29*(2), 202–206.

Sun, H., E. Kunze, and A. Williams III (1996), Vertical heat-flux measurements from a neutrally buoyant float, *Journal of physical oceanography*, *26*(6), 984–1001.

Sun, O. M., and R. Pinkel (2012), Energy transfer from high-shear, low-frequency internal waves to high-frequency waves near kaena ridge, hawaii, *Journal of Physical Oceanography*, *42*(9), 1524–1547.

Thomas, L. N., A. Tandon, and A. Mahadevan (2008), Submesoscale processes and dynamics, *Ocean modeling in an Eddying Regime*, *177*, 17–38.

Thompson, A. F., A. Lazar, C. Buckingham, A. C. N. Garabato, G. M. Damerell, and K. J. Heywood (2016), Open-ocean submesoscale motions: A full seasonal cycle of mixed layer instabilities from gliders, *Journal of Physical Oceanography*, *46*(4), 1285–1307.

van Haren, H., G. Voet, M. H. Alford, B. Fernández-Castro, A. C. N. Garabato, B. L. Wynne-Cattanach, H. Mercier, and M.-J. Messias (), Near-slope turbulence in a rockall canyon, *Deep Sea Res. Part I Oceanogr. Res. Pap.*

Wenegrat, J. O., and L. N. Thomas (2020), Centrifugal and symmetric instability during ekman adjustment of the bottom boundary layer, *Journal of Physical Oceanography*, *50*(6), 1793–1812.

Wenegrat, J. O., J. Callies, and L. N. Thomas (2018), Submesoscale baroclinic instability in the bottom boundary layer, *Journal of Physical Oceanography*, *48*(11), 2571–2592.

Williams 3rd, A. J., J. S. Tochko, R. L. Koehler, W. D. Grant, T. F. Gross, and C. V. Dunn (1987), Measurement of turbulence in the oceanic bottom boundary layer with an acoustic current meter array, *Journal of Atmospheric and Oceanic Technology*, *4*(2), 312–327.

Winters, K. (2015), Tidally driven mixing and dissipation in the stratified boundary layer above steep submarine topography, *Geophysical Research Letters*, *42*(17), 7123–7130.

Yu, X., A. C. Naveira Garabato, A. P. Martin, C. E. Buckingham, L. Brannigan, and Z. Su (2019), An annual cycle of submesoscale vertical flow and restratification in the upper ocean, *Journal of Physical Oceanography*, *49*(6), 1439–1461.

Zhang, X., and M. Nikurashin (2020), Small-scale topographic form stress and local dynamics of the southern ocean, *Journal of Geophysical Research: Oceans*, *125*(8), e2019JC015,420.